

Modeling the Size Effect on the Mechanical Behavior of Functionally Graded Curved Micro/Nanobeam

Seyyed Amirhosein Hosseini^{1*}, O. Rahmani²

¹ Department of Industrial, Mechanical and Aerospace engineering, Buein Zahra Technical University, Buein Zahra, Qazvin, Iran

² Smart Structures and New Advanced Materials Laboratory Department of Mechanical Engineering, University of Zanjan, Zanjan, Iran

ABSTRACT

The size effect on the free vibration and bending of a curved FG micro/nanobeam is studied in this paper. Using the Hamilton principle the differential equations and boundary conditions is derived for a nonlocal Euler-Bernoulli curved micro/nanobeam. The material properties vary through radius direction. Using the Navier approach an analytical solution for simply supported boundary conditions is obtained where the power index law of FGM, the curved micro/nanobeam opening angle, the effect of aspect ratio and nonlocal parameter on natural frequencies and the radial and tangential displacements were analyzed. It is concluded that increasing the curved micro/nanobeam opening angle results in decreasing and increasing the frequencies and displacements, respectively. To validate the natural frequencies of curved nanobeam, when the radius of it approaches to infinity, is compared with a straight FG nanobeam and showed a good agreement.

Keywords: Curved Nanobeam; Functionally Graded Material (FGM); Free Vibration; Bending; Nonlocal Elasticity

1. Introduction

Many fields of science and industry such as civil and mechanical engineering, human health science and aerospace industry are significantly affected by nanotechnology and as a result various investigations are conducted to enhance the physical, electrical and mechanical performance of the nanodevices and nanostructures^[1]. Accurate understanding of nanostructure's mechanical behavior is strongly required to design and manufacture these sort of structures. Conducted investigations in this field showed that the mechanical behavior of nanostructure differs with those of macrostructures. The nonlocal theory of Eringen is the most common theory used by researcher to study the nanostructures mechanical behavior. According to this theory the stress at point x not only depends on the strain of that point, but also depends on the strain of all other points. Numerous investigations are done to study the vibrational behavior of nanostructures using the nonlocal theory. In one study conducted by Soltani *et al.* the transverse vibration of a single-walled carbon nanotube (SWCNT) is modeled by the nonlocal Euler-Bernoulli and Timoshenko beam theory^[2].

Superior properties of nanocomposites has led them to being largely used in nanotechnology, however the distinct interface with sudden variation in material properties has decreased their reliability^[3]. Functionally Graded Materials (FGM) can solve this problem due to their continuous variation in material properties of the constituents^[4-9]. Hence this type of materials are widely used as FG nanobeams and FG nanoplates which are deployed in various industries as aeronautic, manufacturing, nuclear engineering and reactors^[10].

¹ Corresponding author at: Department of Industrial, Mechanical and Aerospace engineering, Buein Zahra Technical University, Buein Zahra, Qazvin, Iran . Tel.: +989127839315

E-mail address: hosseini@znu.ac.ir (Seyyed Amirhosein Hosseini)

Nazemnezhad *et al* studied the nonlinear free vibration FG nanobeams with immovable ends by using the nonlocal elasticity within the frame work of Euler–Bernoulli beam theory with von kármán type nonlinearity. They concluded that while the linear frequency ratios are independent of the gradient index, the nonlinear frequency ratios vary with the gradient index^[11]. Salehipour *et al.* used a three-dimensional (3-D) nonlocal elasticity theory of Eringen, to propose closed-form solutions for in-plane and out-of-plane free vibration of simply supported FG rectangular micro/nano plates. They derived natural frequencies of FG micro/nano plate for different values of nonlocal parameter and gradient inde of material properties^[12]. Niknam and Aghdam have obtained a closed form solution for nonlinear vibration and buckling behavior of Euler-Bernoulli based FG nanobeam by using nonlocal theory^[4]. Elather *et al.* used an efficient finite element model for vibration analysis of a nonlocal Euler-Bernoulli nanobeam^[13]. The static- buckling behavior of functionally graded nanobeams as a core structure of micro and nano electro mechanical systems is analyzed by Eltaher *et al.* Equilibrium equations have been derived by applying the principle of virtual displacement. The significance role of parameters such as material gradient index, boundary conditions and nonlocal effect on the static- buckling behavior of FG nanobeam was concluded^[14]. In one other study they investigate static and buckling behavior of nonlocal FG Timoshenko nanobeam which showed the importance of the material distribution profile effect on the buckling and bending behavior of nanobeams^[15]. Kiani *et al.* proposed a mathematical model for functionally graded nano beam moving with constant velocity. They have investigated the effect of power-law parameter, small-scale parameter and length of the functionally graded nanobeam, on the frequencies and stability of the moving nanobeam^[16]. Uymaz studied the forced vibration of FG nanobeams based on the nonlocal elasticity theory. the solution is derived using Navier method for various shear deformation theories^[17].

The structural analysis of curved beam and curved nanobeam is strongly required in design of various engineering structures so numerous investigations are nowadays conducted to analyze these types of beams and nanobeam^[18]. Wang *et al.* conducted a study to analyze the free vibration of nanorings/arches using the Eringen nonlocal theory which considers the small scale effect^[19]. The dynamic behavior of curved nanobeam was studied by Farshi *et al.* It worth mentioning that they considered the small scale effect in their research. Their results showed that there is a significant difference between the results obtained from their proposed model and those of classical theories^[20]. Medina *et al.* studied the asymmetric buckling of a shallow initially curved microbeam which is subjected to distributed nonlinear deflection-dependent electrostatic forced. Their obtained results were in good agreement with those of direct numerical analysis^[21].

According to the literature review there is no investigation about free vibration and bending analysis of functionally graded curved nanobeam using nonlocal elasticity theory and majority of the conducted literatures were about straight nanobeams and this paper aimed to fill this gap. In this paper free vibration and bending of a curved FG nanobeam is analyzed. The differential equations and boundary conditions are obtained using Hamilton principle and also using the nonlocal theory the equation of motions is derived. Navier approach is employed to obtain an analytical solution for simply supported boundary conditions where the power index law of FGM, the curved nanobeam opening angle, the effect of aspect ratio and nonlocal parameter on natural frequencies and the radial and tangential displacements were assessed. As a result it was concluded that increasing the curved nanobeam opening angle results in decreasing and increasing the frequencies and displacements, respectively. For the sake of validation, the vibration of curved nanobeam when its radius extends to infinity was obtained and compared with those of straight one which showed an excellent agreement.

2. Governing Equation

Based on Euler-Bernoulli theory for curved beams it is assumed that the perpendicular plane to the cross-section before deformation should remain perpendicular after deformation. The radial displacement u and tangential displacement w are evaluated as follows:

$$w(\theta, r, t) = w_0(\theta, t) + \frac{z}{R} \left(w_0(\theta, t) + \frac{\partial u_0(\theta, t)}{\partial \theta} \right) \quad (1)$$

$$u(\theta, r, t) = -u_0(\theta, t)$$

Where u_0 and w_0 denotes the radial and tangential displacement at any points of the middle plane of curved nanobeam, respectively and R shows the radius of curved nanobeam. **Figure 1** shows a schematic of functionally graded curved beam.

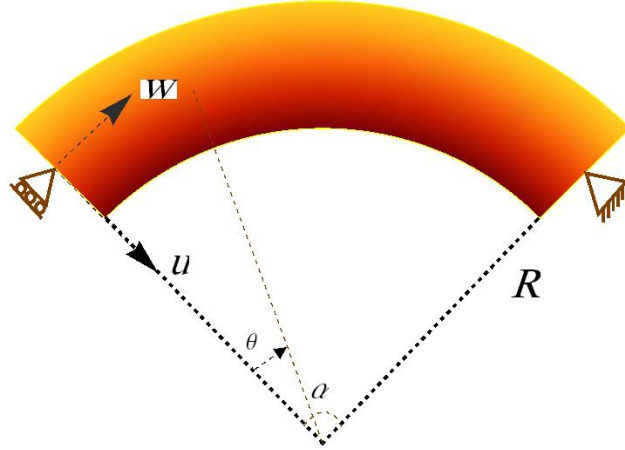


Figure 1; Schematic of functionally graded curved beam.

Strain in an element of curved nanobeam is as follows:

$$\varepsilon_{xx} = \varepsilon_{xx}^0 + z k_x^0 \quad (2)$$

Where ε_{xx} and k_x denotes the tensional and bending strains respectively, which are given as follows:

$$\varepsilon_{xx}^0 = \frac{1}{R} \left(-u_0(\theta, t) + \frac{\partial w_0(\theta, t)}{\partial \theta} \right) \quad (3)$$

$$k_x^0 = \frac{1}{R^2} \left(\frac{\partial w_0(\theta, t)}{\partial \theta} + \frac{\partial^2 u_0(\theta, t)}{\partial \theta^2} \right) \quad (4)$$

The governing equations and boundary conditions are derived using the Hamilton principle:

$$\int_0^t \delta(U - T + V) dt = 0 \quad (5)$$

Where in Equation (4) δU , δT and δV indicate the strain energy, the bending energy and the performed work by external forces, respectively which are calculated as follows:

$$\delta U = \int_V \sigma_{ij} \delta \varepsilon_{ij} dV = \int_V (\sigma_{xx} \delta \varepsilon_{xx}) dV = \int_0^\alpha (N (\delta \varepsilon_{xx}^0) + M (\delta k_x^0)) R d\theta \quad (6)$$

Where the resultant of normal force and bending moment are given as:

$$N = \int_A \sigma_{xx} dA, \quad M = \int_A \sigma_{xx} z dA \quad (7)$$

The first variation for kinetic energy is defined as:

$$\delta T = \int_0^\alpha \left[I_0 \left(\frac{\partial u_0}{\partial t} \frac{\partial \delta u_0}{\partial t} + \frac{\partial w_0}{\partial t} \frac{\partial \delta w_0}{\partial t} \right) + \frac{I_1}{R} \left(2 \frac{\partial w_0}{\partial t} \frac{\partial \delta w_0}{\partial t} + \frac{\partial w_0}{\partial t} \frac{\partial^2 \delta u_0}{\partial t \partial \theta} + \frac{\partial^2 u_0}{\partial t \partial \theta} \frac{\partial \delta w_0}{\partial t} \right) + \right. \\ \left. \frac{I_2}{R^2} \left(\frac{\partial w_0}{\partial t} \frac{\partial \delta w_0}{\partial t} + \frac{\partial w_0}{\partial t} \frac{\partial^2 \delta u_0}{\partial t \partial \theta} + \frac{\partial^2 u_0}{\partial \theta \partial t} \frac{\partial \delta w_0}{\partial t} + \frac{\partial^2 u_0}{\partial t \partial \theta} \frac{\partial^2 \delta u_0}{\partial t \partial \theta} \right) \right] R d\theta \quad (8)$$

Where I_0, I_1 and I_2 are as follows:

$$(I_0, I_1, I_2) = \int_A \rho(z) (1, z, z^2) dA \quad (9)$$

The first variation for the performed work is expressed as:

$$\delta V = -b \int_0^\alpha (f \delta u + p \delta w) R d\theta \quad (10)$$

Where f and p shows the radial and tangential distributed force, respectively. Substituting Equations (6), (8) and (10) into Equation (5) the following equations are obtained:

$$-\frac{\partial N}{\partial \theta} - \frac{1}{R} \frac{\partial M}{\partial \theta} - p R = \left(-I_0 \frac{\partial^2 w_0}{\partial t^2} - \frac{I_1}{R} \left(\frac{\partial^2 w_0}{\partial t^2} + \frac{\partial^3 u_0}{\partial \theta \partial t^2} \right) - \frac{I_2}{R^2} \left(\frac{\partial^2 w_0}{\partial t^2} + \frac{\partial^3 u_0}{\partial \theta \partial t^2} \right) \right) R \quad (11)$$

$$-N + \frac{\partial^2 M}{R \partial \theta^2} - f R = \left(-I_0 \frac{\partial^2 u_0}{\partial t^2} + \frac{I_1}{R} \frac{\partial^3 w_0}{\partial \theta \partial t^2} + \frac{I_2}{R^2} \left(\frac{\partial^3 w_0}{\partial \theta \partial t^2} + \frac{\partial^4 u_0}{\partial \theta^2 \partial t^2} \right) \right) R \quad (12)$$

The boundary conditions are as follows:

$$N + \frac{M}{R} = 0 \quad \text{or} \quad w_0 = 0 \quad \text{at} \quad \theta = 0 \quad \text{and} \quad \theta = \alpha \quad (13.a)$$

$$\frac{\partial M}{R \partial \theta} + I_1 \frac{\partial^2 w_0}{\partial t^2} + \frac{I_2}{R} \left(\frac{\partial^2 w_0}{\partial t^2} + \frac{\partial^3 u_0}{\partial \theta \partial t^2} \right) = 0 \quad \text{or} \quad u_0 = 0 \quad \text{at} \quad \theta = 0 \quad \text{and} \quad \theta = \alpha \quad (13.b)$$

$$M = 0 \quad \text{or} \quad \frac{\partial u_0}{\partial \theta} = 0 \quad \text{at} \quad \theta = 0 \quad \text{and} \quad \theta = \alpha \quad (13.c)$$

3. The FGM material properties

It is assumed that the curved nanobeam is a mixture of steel and Alumina where their material properties are given in **Table 1**. According to present method the gradient variation may be chosen arbitrarily, though to simplify the mathematical treatment, it is common for them to be shown as exponential-type dependence. However from an experimental vantage point, it seems constructive to employ a power law gradient. Therefore the effective material properties of the curved nanobeam are obtained by:

$$E_f(z) = (E_c - E_m) \left(\frac{z}{h} + \frac{1}{2} \right)^p + E_m \\ \rho_f(z) = (\rho_c - \rho_m) \left(\frac{z}{h} + \frac{1}{2} \right)^p + \rho_m \quad (14)$$

p denotes the non-negative constant which describes the volume fraction. Subscripts b and t represents the bottom and top of the curved nanobeam respectively. According to aforementioned subscripts when $z = -h/2, E = E_b$ and $z = h/2, E = E_t$. For the sake of simplicity the bottom and the top surface of the FG curved nanobeam is assumed

to be purely steel and purely alumina, respectively. Although such a power-law relation is not approximate, the above power-law relation can be easily dominated using the variation of the volume fraction of steel and alumina from the bottom to the top in experimental tasks. The variation profile of material properties across the thickness of the beam is denoted by p . Based on distribution function, when $p=0$ the material is homogenous.

Properties	Steel	Alumina(Al_2O_3)
E	210(Gpa)	390 (GPa)
ρ	7800 (kg/m^3)	3960 (kg/m^3)

Table1. Material properties of FGM

4. Nonlocal Theory

Based on Eringen nonlocal theory, the stress field at point X does not only depend to the strain of the same point and is also depend to strain of all other points of the body. The aforementioned fact is proven by the atomic theory of lattice dynamic and experimental observation of phonon dispersion. The stress tensor σ at point X is calculated as follows:

$$\bar{\sigma} = \int_{\Omega} K(|X' - X, \tau|) \sigma(X') dX' \quad (15)$$

σ represents the classical, microscopic second Piola-Kirchhoff stress tensor at point X , the kernel function $K(|X' - X, \tau|)$ denotes the nonlocal modulus, $|X' - X|$ is the distance and τ stands for material parameter which depends on internal and external characteristic length. Based on the generalized Hooke's law the macroscopic stress σ at point X in Hookean solid is related to the strain zeta at point X which is as follows:

$$\sigma(X) = C(X) : \varepsilon(X) \quad (16)$$

The fourth-order elasticity tensor which denotes double-dot product is represented by C . Equation (1) and (2) together represent the nonlocal constitutive behavior of Hookean solid. The weighted average of the contributions of the strain field of all points in the body to the stress field at point X is indicated by Equation (1). For the sake of simplicity, an equivalent differential model is used instead of integral constitutive relation, which is evaluated as follows:

$$(1 - \mu \nabla^2) \bar{\sigma} = \sigma, \quad \mu = \tau^2 \ell^2 = e_0^2 a^2 \quad (17)$$

where τ is determined by $\tau = e_0 a / \ell$ where e_0 is a constant which varies based on each material and a and ℓ represents the internal and external characteristic length. The nonlocal parameter which is represented by μ varies in accordance with different materials. For an elastic material in the one dimensional case, the nonlocal constitutive relations may be simplified as (Eringen & Edelen^[22], 1972):

$$\sigma(x) - (e_0 a)^2 \frac{\partial^2 \sigma(x)}{\partial x^2} = E \varepsilon(x) \quad (18)$$

E is the Young's modulus. For Euler-Bernoulli nonlocal FG beam, Eq. (20) can be written as:

$$\sigma_{xx} - \mu \frac{\partial^2 \sigma_{xx}}{\partial x^2} = E(z) \varepsilon_{xx} \quad (19)$$

Considering equation (19) normal force and bending moment resultants of the nonlocal Euler-Bernoulli theory are obtained as follows

$$N - \mu \frac{\partial^2 N}{R^2 \partial \theta^2} = \frac{A}{R} \left(-u + \frac{\partial w}{\partial \theta} \right) - \frac{B}{R^2} \left(\frac{\partial w}{\partial \theta} + \frac{\partial^2 u}{\partial \theta^2} \right) \quad (20)$$

$$M - \mu \frac{\partial^2 M}{R^2 \partial \theta^2} = \frac{B}{R^2} \left(-u + \frac{\partial w}{\partial \theta} \right) + \frac{D}{R^2} \left(\frac{\partial w}{\partial \theta} + \frac{\partial^2 u}{\partial \theta^2} \right) \quad (21)$$

Where A_{xx} , B_x and D_{xx} are extensional, bending-extensional, and bending stiffness coefficients, respectively which are derived as follows:

$$(A, B, D) = \int_A E(z, T) (1, z, z^2) dA \quad (22)$$

After some algebraic manipulations and substituting N and M resultants into Equations (20) and (21) the nonlocal equation of motions becomes follows:

$$\frac{A}{R} \left(-\frac{\partial u_0}{\partial \theta} + \frac{\partial^2 w_0}{\partial \theta^2} \right) + \frac{B}{R^2} \left(2 \frac{\partial^2 w_0}{\partial \theta^2} + \frac{\partial^3 u_0}{\partial \theta^3} - \frac{\partial u_0}{\partial \theta} \right) + \frac{D}{R^3} \left(\frac{\partial^2 w_0}{\partial \theta^2} + \frac{\partial^3 u_0}{\partial \theta^3} \right) + pR + \frac{\mu}{R^2} \left(I_0 R \frac{\partial^4 w_0}{\partial \theta^2 \partial t^2} + I_1 \left(2 \frac{\partial^4 w_0}{\partial \theta^2 \partial t^2} + \frac{\partial^5 u_0}{\partial t^2 \partial \theta^3} \right) + \frac{I_2}{R} \left(\frac{\partial^4 w_0}{\partial \theta^2 \partial t^2} + \frac{\partial^5 u_0}{\partial t^2 \partial \theta^3} \right) - R \frac{\partial^2 p}{\partial \theta^2} \right) = \quad (23)$$

$$I_0 R \frac{\partial^2 w_0}{\partial t^2} + I_1 \left(2 \frac{\partial^2 w_0}{\partial t^2} + \frac{\partial^3 u_0}{\partial t^2 \partial \theta} \right) + \frac{I_2}{R} \left(\frac{\partial^2 w_0}{\partial t^2} + \frac{\partial^3 u_0}{\partial t^2 \partial \theta} \right) \frac{A}{R} \left(-u_0 + \frac{\partial w_0}{\partial \theta} \right) + \frac{B}{R^2} \left(\frac{\partial w_0}{\partial \theta} + 2 \frac{\partial^2 u_0}{\partial \theta^2} - \frac{\partial^3 w_0}{\partial \theta^3} \right) - \frac{D}{R^3} \left(\frac{\partial^3 w_0}{\partial \theta^3} + \frac{\partial^4 u_0}{\partial \theta^4} \right) + Rf + \frac{\mu}{R^2} \left(I_0 R \frac{\partial^4 u_0}{\partial \theta^2 \partial t^2} - I_1 \frac{\partial^5 w_0}{\partial t^2 \partial \theta^3} - \frac{I_2}{R} \left(\frac{\partial^5 w_0}{\partial t^2 \partial \theta^3} + \frac{\partial^6 u_0}{\partial t^2 \partial \theta^4} \right) + R \frac{\partial^2 f}{\partial \theta^2} \right) = \quad (24)$$

$$I_0 R \frac{\partial^2 u_0}{\partial t^2} - I_1 \frac{\partial^3 w_0}{\partial t^2 \partial \theta} - \frac{I_2}{R} \left(\frac{\partial^3 w_0}{\partial t^2 \partial \theta} + \frac{\partial^4 u_0}{\partial t^2 \partial \theta^2} \right)$$

5. The analytical solution for bending and vibration of a curved FG nanobeam

In this section, the equation of motions for bending and free vibration of a simply supported curved nanobeam is solved using an analytical solution. The Navier equation is employed to derive the analytical solution. The known trigonometric displacement functions with unknown coefficients are considered to satisfy the boundary conditions and the differential equations. The following equations indicate the displacement functions.

$$u_0(\theta, t) = \sum_{n=1}^N U_n \sin\left(\frac{n\pi}{\alpha} \theta\right) e^{i\omega_n t} \quad (25)$$

$$w_0(\theta, t) = \sum_{n=1}^{\infty} W_n \cos\left(\frac{n\pi}{\alpha} \theta\right) e^{i\omega_n t} \quad (26)$$

Where $i = \sqrt{-1}$ and ω_n denotes the vibrational frequency and U_n , W_n are unknown Fourier coefficients.

6. Static analysis

For static analysis all the time relevant parameters should be equal to zero. In the present work the radial force f is the only existed force while the p is ignored. The radial force of f is in the form of Fourier expansion which is evaluated as follows:

$$f(\theta) = \sum_{n=1}^N F_n \sin\left(\frac{n\pi}{\alpha}\theta\right) \quad (27)$$

$$F_n = \frac{2}{\alpha} \int_0^{\alpha} f(\theta) \sin\left(\frac{n\pi}{\alpha}\theta\right) d\theta \quad (28)$$

Where F_n denote the Fourier coefficients that are under different loads as follows:

Uniform load:

$$f(\theta) = f_0 R \quad F_n = \frac{4f_0 R}{n\pi}, \quad n = 1, 3, 5, 7, \dots \quad (29)$$

Point load:

$$f(\theta) = F R \delta(\theta - \theta_p) \quad F_n = \frac{2F}{\alpha} \sin\left(\frac{n\pi}{\alpha}\theta_p\right), \quad n = 1, 2, 3, \dots \quad (30)$$

Where f_0 denotes the intensity of the uniform distributed load. The Dirac delta function is represented by $\delta(\cdot)$ and F is the amount of the point load. The location of angular point load of F is shown by θ_p . If it is assumed that the

loading is applied to the middle of the curved nanobeam $f(\theta) = F R \delta\left(\theta - \frac{\alpha}{2}\right)$ the mentioned equation would become as follows:

$$F_n = \frac{2F}{\alpha} \sin\left(\frac{n\pi}{2}\right), \quad n = 1, 2, 3, \dots \quad (31)$$

Substituting Equation (25) and (26) into Equations (26) and (24) the matrix of algebraic equation is obtained as follows:

$$\begin{bmatrix} S_{11}^n & S_{12}^n \\ S_{21}^n & S_{22}^n \end{bmatrix} \begin{bmatrix} U_n \\ W_n \end{bmatrix} = \begin{bmatrix} F_n \lambda_n \\ 0 \end{bmatrix} \quad (32)$$

Where $S_{11}^n, S_{12}^n, S_{21}^n$ and S_{22}^n and λ_n are evaluated as follows:

$$\begin{aligned} S_{11}^n &= -\frac{A}{R^2} - \frac{2B}{R^3} \left(\frac{n\pi}{\alpha}\right)^2 - \frac{D}{R^4} \left(\frac{n\pi}{\alpha}\right)^4 \\ S_{12}^n &= -\frac{A}{R^2} \left(\frac{n\pi}{\alpha}\right) - \frac{B}{R^3} \left(\left(\frac{n\pi}{\alpha}\right) + \left(\frac{n\pi}{\alpha}\right)^3\right) - \frac{D}{R^4} \left(\frac{n\pi}{\alpha}\right)^4 \\ S_{21}^n &= S_{12}^n, \quad S_{22}^n = -\frac{A}{R^2} \left(\frac{n\pi}{\alpha}\right)^2 - \frac{2B}{R^3} \left(\frac{n\pi}{\alpha}\right)^2 - \frac{D}{R^4} \left(\frac{n\pi}{\alpha}\right)^2 \\ \lambda_n &= -\left(1 + \frac{\mu}{R^2} \left(\frac{n\pi}{\alpha}\right)^2\right) \end{aligned} \quad (33)$$

Solving the abovementioned equation results in:

$$U_n = \frac{F_n \lambda_n S_{22}^n}{S_{11}^n S_{22}^n - (S_{12}^n)^2} \quad (34)$$

$$W_n = \frac{-F_n \lambda_n S_{12}^n}{S_{11}^n S_{22}^n - (S_{12}^n)^2} \quad (35)$$

7. Free vibration analysis

All the external forces should be equal to zero for static analysis of curved nanobeam. Substituting equations (25) and (26) into equations (23) and (24) the eigenvalues are obtained as follows:

$$\left(\begin{bmatrix} S_{11}^n & S_{12}^n \\ S_{12}^n & S_{22}^n \end{bmatrix} + \omega_n^2 \begin{bmatrix} M_{11}^n & M_{12}^n \\ M_{12}^n & M_{22}^n \end{bmatrix} \right) \begin{Bmatrix} U_n \\ W_n \end{Bmatrix} = \begin{Bmatrix} 0 \\ 0 \end{Bmatrix} \quad (36)$$

The mass matrix coefficients are as follows:

$$\begin{aligned} M_{11}^n &= I_0 + \frac{I_2}{R^2} \left(\frac{n\pi}{\alpha} \right)^2 + \frac{\mu}{R^2} \left(I_0 \left(\frac{n\pi}{\alpha} \right)^2 + \frac{I_2}{R^2} \left(\frac{n\pi}{\alpha} \right)^4 \right) \\ M_{12}^n &= \frac{I_1}{R} \left(\frac{n\pi}{\alpha} \right) + \frac{I_2}{R^2} \left(\frac{n\pi}{\alpha} \right) + \frac{\mu}{R^2} \left(\frac{I_1}{R} \left(\frac{n\pi}{\alpha} \right)^3 + \frac{I_2}{R^2} \left(\frac{n\pi}{\alpha} \right)^3 \right) \\ M_{22}^n &= I_0 + 2 \frac{I_1}{R} + \frac{I_2}{R^2} + \frac{\mu}{R^2} \left(\left(I_0 + 2 \frac{I_1}{R} + \frac{I_2}{R^2} \right) \left(\frac{n\pi}{\alpha} \right)^2 \right) \end{aligned} \quad (37)$$

8. Numerical results

The numerical solution for free vibration of a curved FG nanobeam is presented in this section. Firstly, our work is validated by previous work and secondly some numerical examples are presented.

9. Validation

According to the obtained equations as the radius of curved nanobeam extends to infinity the resulted frequencies approach to those of straight one. For this purpose the present work is compared with Eltaher work in the first mode of frequency in Table 2, for different nonlocal parameters and also different power low indexes (0, 0.2, 1, and 5). As it is clear the obtained results were in an excellent agreement with those of Eltaher work^[23] that was solved using the Finite Element Method (FEM). It should be noted that the given results were dimensionalized using the $\bar{\omega} = \omega \times L^2 \sqrt{\frac{\rho_c A}{E_c I}}$ relation.

L/h	μ	P=0			P=0.2			P=1			P=5		
		Present	Eltaher <i>et al.</i> [23]		Present	Eltaher <i>et al.</i> [23]		Present	Eltaher <i>et al.</i> [23]		Present	Eltaher <i>et al.</i> [23]	
20	0	9.8594	9.8797		8.6858	8.7200		6.9885	7.0904		5.9370	6.0025	
	1×10^{-12}	9.40622	9.4238		8.2865	8.3175		6.6672	6.7631		5.66411	5.7256	
	2×10^{-12}	9.0102	9.0257		7.9376	7.9661		6.3865	6.4774		5.4256	5.4837	
	3×10^{-12}	8.6603	8.6741		7.6294	7.6557		6.1385	6.2251		5.2449	5.2702	
	4×10^{-12}	8.3483	8.3607		7.3545	7.3791		5.9174	6.0001		5.0271	5.0797	
50	0	9.8679	9.8797		8.6937	8.7115		6.9951	7.0852		5.9421	5.9990	
	1×10^{-12}	9.4143	9.4172		8.2940	8.3114		6.6735	6.7583		5.6689	5.7218	
	2×10^{-12}	9.0180	9.0205		7.9448	7.9613		6.3925	6.4737		5.4302	5.4808	
	3×10^{-12}	8.6678	8.6700		7.6363	7.5620		6.1437	6.2222		5.2194	5.2679	
	4×10^{-12}	8.3555	8.3575		7.3612	7.3762		5.9229	5.9979		5.0314	5.0780	

100	0	9.8692	9.8700	8.6948	8.7111	6.9960	7.0833	5.9428	5.9970
	1×10^{-12}	9.4154	9.4162	8.2951	8.3106	6.6744	6.7577	5.6696	5.7212
	2×10^{-12}	9.0191	9.0197	7.9459	7.9607	6.3934	6.4731	5.4309	5.4803
	3×10^{-12}	8.6689	8.6695	7.6373	7.6515	6.1452	6.2217	5.2201	5.2675
	4×10^{-12}	8.3565	8.3571	7.3622	7.3758	5.9237	5.9976	5.0320	5.0777

Table 2. Dimensionless frequencies for first mode

10. Free vibration results

The numerical solution of a curved FG nanobeam with mentioned material properties of Table 1 is presented in this section. It should be mentioned that the value of natural frequency is found by setting the determinant of the equation (34) to zero. The results are in the forms of $\bar{\omega} = \omega \times L^2 \sqrt{\frac{\rho_c A}{E_c I}}$ where $\bar{\omega}$ denotes the dimensionalized natural frequency of a curved FG nanobeam.

The dimensionalized frequencies of curved FG nanobeam are represented in Table 3 for the power law index (p) of zero. In other words, the dimensionalized frequency of a curved FG nanobeam for different values of nonlocal parameter, various opening angles of curved nanobeam along a constant length and different ratios of thickness is presented in **Table 3**. **Tables 4 to 8** illustrate the results of a curved FG nanobeam vibration for different power law indexes of 0.1, 0.2, 1, 5 and 10.

L/h	μ (nm ³)	opening angle (α)								
		$\frac{\pi}{18}$	$\frac{\pi}{9}$	$\frac{\pi}{6}$	$\frac{\pi}{4}$	$\frac{\pi}{3}$	$\frac{\pi}{2}$	$\frac{2\pi}{3}$	$\frac{3\pi}{4}$	
10	0	9.783	9.648	9.425	8.938	8.286	6.5912	4.542	3.439	
		7	0	2	0	3		3	6	
	1	9.333	9.204	8.991	8.527	7.905	6.2882	4.333	3.281	
		9	5	9	1	4		5	5	
	2	8.940	8.817	8.613	8.168	7.572	6.0235	4.1511	3.143	
		9	0	4	1	6		4.1511	3	
	3	8.593	8.474	8.278	7.850	7.278	5.7896	3.989	3.021	
		8	6	9	9	5		9	3	
	4	8.284	8.169	7.980	7.568	7.016	5.5810	3.846	2.912	
		2	3	6	1	3		1	4	
	25	0	9.817	9.681	9.458	8.970	8.316	6.6159	4.559	3.451
			5	6	5	3	9		0	9
1		9.366	9.236	9.023	8.557	7.934	6.3118	4.349	3.293	
		1	6	6	9	5		4	3	
2		8.971	8.847	8.643	8.197	7.600	6.0461	4.166	3.154	
		8	7	8	6	5	2	3	6	
3		8.623	8.504	8.308	7.879	7.879	5.8113	4.004	3.032	
		5	2	1	3	3		5	1	
4		8.312	8.197	8.008	7.595	7.595	5.6019	3.860	2.922	
		8	8	8	4	4		2	9	
50		0	9.822	9.686	9.463	8.974	8.321	6.6195	4.561	3.453
			3	5	3	9	3		4	7

100	1	9.370	9.241	9.028	8.562	7.938	6.3152	4.351	3.294	
		8	2	2	3	7		7	9	
	2	8.976	8.852	8.648	8.201	7.604	6.0493	4.168	3.156	
		3	1	1	8	5		5	2	
	3	8.627	8.508	8.312	7.883	7.309	5.8144	4.006	3.033	
		7	4	3	4	2		6	7	
	4	8.316	8.201	8.012	7.559	7.045	5.6049	3.862	2.924	
		9	9	8	3	9		3	4	
	100	0	9.823	9.687	9.464	8.976	8.322	6.6204	4.562	3.452
			5	7	4	1	4		0	1
		1	9.371	9.242	9.029	8.563	7.939	6.3160	4.352	3.295
			9	3	3	4	8		3	4
		2	8.977	8.853	8.649	8.202	7.605	6.0501	4.169	3.156
			4	2	2	9	5		0	6
		3	8.628	8.509	8.313	7.884	7.310	5.8152	4.007	3.034
			8	5	4	4	2		2	1
4		8.317	8.202	8.013	7.600	7.046	5.6057	3.862	2.924	
		9	9	9	3	8		8	8	

Table 3. The variation of dimensionless frequencies versus opening angle, nonlocal parameter and aspect ratio for simply supported curved beam ($\rho=0$)

Observing the results of Tables 3 to 8 it is concluded that as the nonlocal parameter increases the value of dimensionalized frequency decreases and as the opening angles increases from to the dimensionalized frequency decreases dramatically. Thorough analyzing the aforementioned tables shows that as the opening angles of curved FG nanobeam (in the constant length of curved nanobeam) decreases, the frequency of curved FG nanobeam approaches to those of straight nanobeam in low value of opening angles. It is clear that as the ratio and aspect ratio increases the dimensionalized frequency slightly increases. The amount of increasing reaches to zero as the ratio increases. This is due to this fact that increasing the ratio of the Euler-Bernoulli beam theory concludes the more accurate results. It should be mentioned that when the curved FG nanobeam opening angle increases from to the maximum differences in amount of frequencies occurs. Also comparing the Tables 3 to 8 shows that as the power index law increases, the amount of frequency reduces which has lower slope when the power index law increases from 5 to 10.

L/h	μ (nm ²)	opening angle (α)							
		$\pi/18$	$\pi/9$	$\pi/6$	$\pi/4$	$\pi/3$	$\pi/2$	$2\pi/3$	$3\pi/4$
10	0	9.1109	8.9786	8.7657	8.3056	7.6948	6.1159	4.2144	3.1918
		7	1	0	1	7	2	1	5
	1	8.6921	8.5658	8.3627	7.9237	7.3411	5.8347	4.0206	3.0451
		3	4	2	9	3	6	7	1
	2	8.3262	8.2052	8.0106	7.5902	7.0320	5.5891	3.8514	2.9169
		0	3	6	0	7	2	0	2
	3	8.0029	7.8866	7.6996	7.2954	6.7590	5.3721	3.7018	2.8036
		0	3	2	9	3	1	6	6
	4	7.7145	7.6024	7.4222	7.0326	6.5155	5.1785	3.5684	2.7026
		6	8	1	3	0	5	8	4

25	0	9.1471	9.0181	8.8080	8.3505	7.7401	6.1551	4.2412	3.2116	
		7	8	5	7	8	5	6	0	
	1	8.7266	8.6036	8.4031	7.9666	7.3843	5.8721	4.0462	3.0639	
		6	0	3	8	5	8	8	5	
	2	8.3592	8.2414	8.0493	7.6312	7.0734	5.6249	3.8759	2.9349	
		8	0	7	9	8	7	4	6	
	3	8.0347	7.9214	7.7368	7.3349	6.7988	5.4065	3.7254	2.8210	
		0	0	2	8	3	6	4	0	
	4	7.7452	7.6359	7.4580	7.0707	6.5538	5.2117	3.5912	2.7193	
		1	9	7	0	7	7	2	6	
	50	0	9.1531	9.0252	8.8161	8.3597	7.7498	6.1639	4.2473	3.2160
			0	9	7	8	7	2	5	7
		1	8.7323	8.6103	8.4108	7.9754	7.3935	5.8805	4.0520	3.0682
			2	8	7	6	9	5	9	2
		2	8.3647	8.2478	8.0567	7.6397	7.0823	5.6329	3.8815	2.9390
			0	9	8	0	3	9	5	3.8815
3		8.0399	7.9276	7.7439	7.3430	6.8073	5.4142	3.7307	2.8249	
		1	4	5	7	4	7	9	3	
4		7.7502	7.6420	7.4649	7.0785	6.5620	5.2192	3.5963	2.7231	
		3	1	4	0	7	0	7	5	
100		0	9.1549	9.0276	8.8190	8.3632	7.7536	6.1674	4.2498	3.2179
			0	9	9	9	8	9	5	0
		1	8.7340	8.6126	8.4136	7.9788	7.3972	5.8839	4.0544	3.0699
			4	7	6	1	3	6	8	6
		2	8.3663	8.2500	8.0594	7.6429	7.0858	5.6362	3.8837	2.9407
			4	8	5	1	2	5	9	2
	3	8.0414	7.9297	7.7465	7.3461	6.8106	5.4174	3.7329	2.8265	
		9	4	2	5	8	0	9	4	
	4	7.7517	7.6440	7.4674	7.0814	6.5653	5.2222	3.5984	2.7247	
		6	4	1	7	0	1	9	0	

Table 4. The variation of dimensionless frequencies versus opening angle, nonlocal parameter and aspect ratio for simply supported curved beam ($\rho=0.1$)

L/h	$\mu(\text{nm}^2)$	opening angle (α)							
		$\frac{\pi}{18}$	$\frac{\pi}{9}$	$\frac{\pi}{6}$	$\frac{\pi}{4}$	$\frac{\pi}{3}$	$\frac{\pi}{2}$	$\frac{2\pi}{3}$	$\frac{3\pi}{4}$
10	0	8.6073	8.4781	8.2733	7.8342	7.2545	5.7624	3.9703	3.0072
		8	6	1	5	6	4	4	7
	1	8.2116	8.0884	7.8929	7.4741	6.9210	5.4975	3.7878	2.8690
		9	1	7	0	6	3	2	2
	2	7.8659	7.7478	7.5606	7.1594	6.6296	5.2660	3.6283	2.7482
		8	9	8	4	9	9	5	4
	3	7.5605	7.4470	7.2671	6.8814	6.3722	5.0616	3.4874	2.6415
		6	6	1	5	7	2	7	3

25	4	7.2881	7.1787	7.0052	6.6335	6.1426	4.8792	3.3618	2.5463
		6	4	8	2	8	5	2	5
	0	8.6448	8.5212	8.3211	7.8870	7.3089	5.8107	4.0037	3.0318
		7	8	7	0	9	5	2	2
	1	8.2474	8.1295	7.9386	7.5244	6.9729	5.5436	3.8196	2.8924
		5	4	3	2	8	2	6	5
	2	7.9002	7.7872	7.6044	7.2076	6.6794	5.3102	3.6588	2.7706
		4	9	2	4	3	4	6	8
3	7.5934	7.4849	7.3091	6.9277	6.4200	5.1040	3.5167	2.6631	
	9	3	5	8	7	5	9	0	
4	7.3199	7.2152	7.0458	6.6781	6.1887	4.9201	3.3900	2.5671	
	0	5	1	8	6	6	8	5	
50	0	8.6514	8.5297	8.3313	7.8990	7.3220	5.8228	4.0122	3.0380
		5	9	7	8	2	7	2	8
	1	8.2537	8.1376	7.9483	7.5359	6.9854	5.5551	3.8277	2.8984
		2	6	6	5	2	8	7	1
	2	7.9062	7.7950	7.6137	7.2186	6.6913	5.3213	3.6666	2.7763
		5	7	5	9	4	1	2	9
	3	7.5992	7.4924	7.3181	6.9384	6.4315	5.1146	3.5242	2.6685
		6	0	2	0	2	9	6	9
4	7.3254	7.2224	7.0544	6.6884	6.1998	4.9304	3.3972	2.5724	
	7	6	5	1	0	1	8	4	
100	0	8.6536	8.5329	8.3353	7.9040	7.3275	5.8281	4.0159	3.0408
		1	4	8	8	6	6	6	3
	1	8.2557	8.1406	7.9521	7.5407	6.9907	5.5602	3.8313	2.9010
		9	6	9	1	0	3	4	3
	2	7.9082	7.7979	7.6174	7.2232	6.6964	5.3261	3.6700	2.7789
		3	5	1	6	0	4	5	0
	3	7.6011	7.4951	7.3216	6.9427	6.4363	5.1193	3.5275	2.6710
		7	7	4	9	9	4	4	0
4	7.3273	7.2251	7.0578	6.6926	6.2044	4.9348	3.4004	2.5747	
	0	2	4	4	9	9	5	7	

Table 5. The variation of dimensionless frequencies versus opening angle, nonlocal parameter and aspect ratio for simply supported curved beam ($p=0.2$)

L/h	$\mu(\text{nm}^2)$	opening angle (α)							
		$\pi/18$	$\pi/9$	$\pi/6$	$\pi/4$	$\pi/3$	$\pi/2$	$2\pi/3$	$3\pi/4$
10	0	6.91423	6.80074	6.62749	6.26441	5.79208	4.59134	3.16089	2.39413
	1	6.59637	6.48810	6.32282	5.97642	5.52581	4.38027	3.01558	2.28407
	2	6.31867	6.21495	6.05663	5.72482	5.29318	4.19586	2.88863	2.18791
	3	6.07332	5.97364	5.82146	5.50253	5.08765	4.03295	2.77647	2.10296
	4	5.85450	5.75841	5.61172	5.30428	4.90434	3.88764	2.67643	2.02719

25	0	6.95155	6.84824	6.68377	6.33033	5.86274	4.65697	3.20764	2.42897
	1	6.63198	6.53341	6.37651	6.03932	5.59322	4.44288	3.06017	2.31730
	2	6.35278	6.25836	6.10806	5.78507	5.35775	4.25584	2.93134	2.21975
	3	6.10611	6.01536	5.87090	5.56044	5.14971	4.09059	2.81752	2.13356
	4	5.88611	5.79863	5.65937	5.36010	4.96417	3.94321	2.71601	2.05669
50	0	6.95905	6.85922	6.69782	6.34792	5.88232	4.67591	3.22135	2.43921
	1	6.63913	6.54389	6.38991	6.05610	5.61190	4.46095	3.07326	2.32708
	2	6.35963	6.26840	6.12090	5.80114	5.37565	4.27315	2.94388	2.22911
	3	6.11269	6.02500	5.88324	5.57589	5.16692	4.10723	2.82957	2.14256
	4	5.89246	5.80793	5.67127	5.37499	4.98076	3.95925	2.72762	2.06536
100	0	6.96186	6.86378	6.70395	6.35587	5.89135	4.68481	3.22784	2.44406
	1	6.64181	6.54824	6.39576	6.06368	5.62051	4.46944	3.07945	2.33171
	2	6.36219	6.27257	6.1265	5.80841	5.38389	4.28128	2.94981	2.23354
	3	6.11516	6.02901	5.88862	5.58288	5.17485	4.11504	2.83527	2.14682
	4	5.89483	5.81179	5.67646	5.38173	4.98840	3.96678	2.73312	2.06947

Table 6. The variation of dimensionless frequencies versus opening angle, nonlocal parameter and aspect ratio for simply supported curved beam ($\rho=1$)

L/h	$\mu(\text{nm}^2)$	opening angle (α)							
		$\frac{\pi}{18}$	$\frac{\pi}{9}$	$\frac{\pi}{6}$	$\frac{\pi}{4}$	$\frac{\pi}{3}$	$\frac{\pi}{2}$	$\frac{2\pi}{3}$	$\frac{3\pi}{4}$
10	0	5.87909	5.78563	5.64091	5.33500	4.93482	3.91309	2.69320	2.03924
	1	5.60882	5.51965	5.38159	5.08974	4.70796	3.73319	2.56939	1.94550
	2	5.37269	5.28728	5.15503	4.87547	4.50976	3.57603	2.46122	1.86359
	3	5.16408	5.08199	4.95487	4.68616	4.33465	3.43718	2.36566	1.79123
	4	4.97802	4.89888	4.77634	4.51732	4.17848	3.31334	2.28043	1.72669
25	0	5.90679	5.82028	5.68164	5.3826	4.98599	3.96129	2.72828	2.06574
	1	5.63525	5.55271	5.42045	5.13515	4.75678	3.77919	2.60285	1.97077
	2	5.39801	5.31894	5.19225	4.91896	4.55652	3.62009	2.49328	1.88780
	3	5.18841	5.11242	4.99064	4.72797	4.37960	3.47952	2.39647	1.81450
	4	5.00147	4.92822	4.81083	4.55762	4.22180	3.35416	2.31012	1.74913
50	0	5.91219	5.82802	5.69148	5.39487	4.99969	3.97472	2.73821	2.07326
	1	5.64040	5.56010	5.42983	5.14686	4.76985	3.79199	2.61233	1.97795
	2	5.40294	5.32602	5.20124	4.93018	4.56904	3.63236	2.50235	1.89468
	3	5.19315	5.11922	4.99928	4.73875	4.39163	3.49132	2.40519	1.82111
	4	5.00605	4.93478	4.81916	4.56802	4.23341	3.36553	2.31853	1.75550
100	0	5.91416	5.83117	5.69568	5.40032	5.00590	3.98092	2.74283	2.07676
	1	5.64228	5.56310	5.43384	5.15206	4.77577	3.79791	2.61673	1.98129
	2	5.40474	5.32890	5.20508	4.93516	4.57472	3.63802	2.50657	1.89788
	3	5.19489	5.12199	5.00298	4.74354	4.39709	3.49676	2.40924	1.82419
	4	5.00772	4.93745	4.82272	4.57263	4.23866	3.37077	2.32244	1.75846

Table 7. The variation of dimensionless frequencies versus opening angle, nonlocal parameter and aspect ratio for simply supported curved beam ($p=5$)

L/h	$\mu(\text{nm}^2)$	opening angle (α)							
		$\frac{\pi}{18}$	$\frac{\pi}{9}$	$\frac{\pi}{6}$	$\frac{\pi}{4}$	$\frac{\pi}{3}$	$\frac{\pi}{2}$	$\frac{2\pi}{3}$	$\frac{3\pi}{4}$
10	0	5.62040	5.53490	5.39999	5.11165	4.73169	3.75564	2.58573	1.95782
	1	5.36202	5.28045	5.15175	4.87666	4.51416	3.58299	2.46686	1.86782
	2	5.13628	5.05815	4.93486	4.67136	4.32412	3.43215	2.36301	1.78919
	3	4.93685	4.86175	4.74325	4.48997	4.15622	3.29888	2.27126	1.71971
	4	4.75898	4.68658	4.57235	4.3282	4.00648	3.18003	2.18943	1.65775
25	0	5.64399	5.56288	5.43182	5.14778	4.76992	3.79117	2.61150	1.97730
	1	5.38452	5.30714	5.18211	4.91113	4.55064	3.61688	2.49144	1.88640
	2	5.15784	5.08372	4.96395	4.70437	4.35906	3.46461	2.38656	1.80699
	3	4.95757	4.88633	4.77121	4.52171	4.18980	3.33009	2.29389	1.73683
	4	4.77895	4.71027	4.59930	4.35879	4.03885	3.21011	2.21124	1.67425
50	0	5.64827	5.56864	5.4389	5.15639	4.77941	3.80038	2.6183	1.98247
	1	5.38861	5.31264	5.18886	4.91934	4.55969	3.62567	2.49794	1.89133
	2	5.16175	5.08898	4.97042	4.71224	4.36773	3.47303	2.39278	1.81171
	3	4.96133	4.89138	4.77742	4.52927	4.19814	3.33818	2.29987	1.74136
	4	4.78258	4.71515	4.60529	4.36609	4.04689	3.21791	2.21701	1.67862
100	0	5.64973	5.57084	5.44177	5.16004	4.78354	3.80448	2.62136	1.98479
	1	5.39000	5.31474	5.19160	4.92283	4.56363	3.62958	2.50085	1.89355
	2	5.16309	5.09100	4.97304	4.71558	4.37151	3.47678	2.39557	1.81383
	3	4.96262	4.89332	4.77994	4.53248	4.20177	3.34178	2.30255	1.74340
	4	4.78381	4.71702	4.60772	4.36918	4.05038	3.22138	2.21959	1.68059

Table 8. The variation of dimensionless frequencies versus opening angle, nonlocal parameter and aspect ratio for simply supported curved beam ($p=10$)

The variation of dimensionalized frequencies versus power law index for opening angles of $\frac{\pi}{18}$, $\frac{\pi}{4}$, $\frac{\pi}{2}$ and $\frac{2\pi}{3}$ and nonlocal parameters of 0, 1, 2 and 3 (nm^2) are illustrated in Figure (2-a) to (2-d). Comparing the aforementioned figures it is illustrated that increasing the power law index up to 2 ($p < 2$) results in a drastic decreasing in dimensionalized frequencies while after $p > 2$ the intensity of its decreasing trends reduces. It should be noted that as the nonlocal parameter increases the amount of dimensionalized frequencies reduces which has the dramatic reduction as the opening angle increases.

The variation of dimensionalized frequencies versus first six vibration modes for different nonlocal parameters of 0, 1, 2, 3 and 4, the opening angles of $\frac{\pi}{9}$, $\frac{\pi}{2}$, $\frac{2\pi}{3}$ and $\frac{3\pi}{4}$, and the power law index of ($p=1$) is illustrated in Figures (3-a) to (3-d). As it was expected increasing the mode number results in the increasing of the dimensionalized natural frequency. It worth mentioning that as the mode numbers increases the difference between the value of frequencies in the classical and nonlocal theory also increases. It was also seen that increasing the curved FG nanobeam opening angles tends to slightly reduce the value of frequencies.

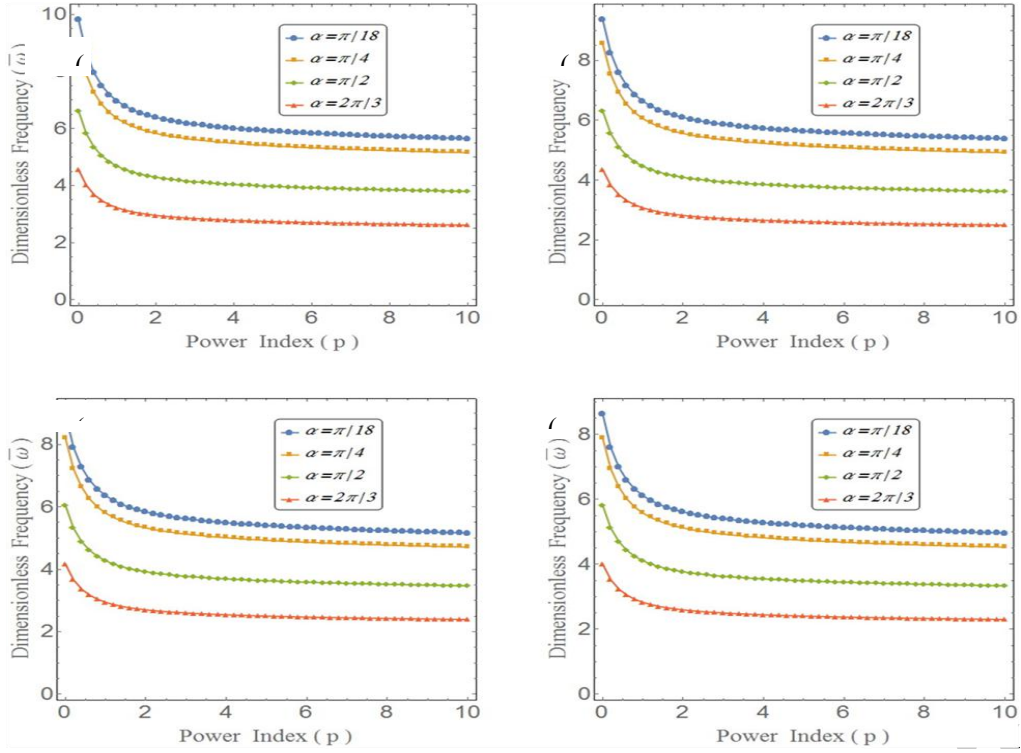


Figure 2; The variation of dimensionalized frequencies versus power law index for opening angles of $\frac{\pi}{18}$, $\frac{\pi}{4}$, $\frac{2\pi}{3}$ and $\frac{2\pi}{3}$ and nonlocal parameters of 0(a), 1(b), 2(c) and 3(d) (nm^2).

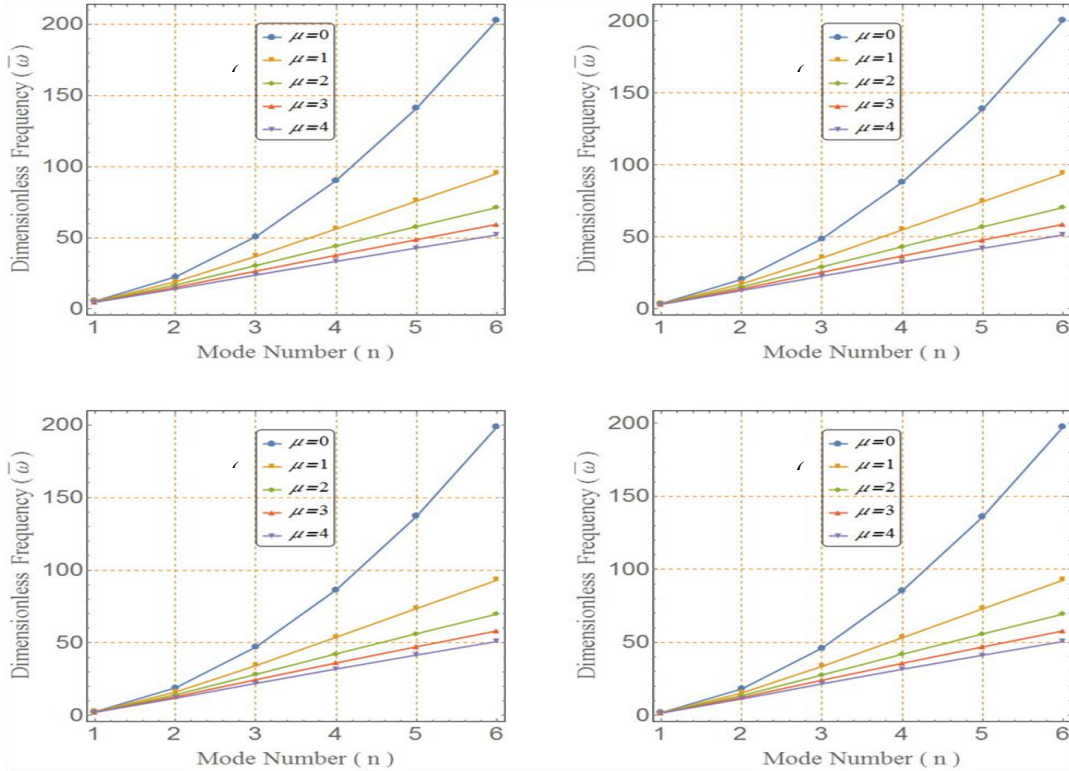


Figure 3; The variation of dimensionalized frequencies versus first six vibration modes for different nonlocal parameters of 0, 1, 2, 3 and 4(nm^2), the opening angles of $\frac{\pi}{9}$ (a), $\frac{\pi}{2}$ (b), $\frac{2\pi}{3}$ (c) and $\frac{3\pi}{4}$ (d).($p=1$).

11. Bending analysis

The maximum center line radial displacement which is under the uniform load for the power law indexes of 0, 0.1, 1 and 10, different nonlocal parameters, and different opening angles of curved FG nanobeam is represented in **Table 9**. The maximum displacement is shown as $\bar{u}_n = \frac{100E_c I}{f_0 R^4 \alpha^4} u_n \left(\frac{\alpha}{2}\right)$ where \bar{u}_n denotes the dimensionalized radial displacement. Observing the mentioned table, it is concluded that increasing the nonlocal parameters increase the dimensionalized radial displacement. Also as the opening angles increases the dimensionalized radial displacement has the similar trend. It should be noted that when the opening angle increases from this to that results in the maximum rate of dimensionalized frequency occurs. The h ratio is equal to 50 in this table.

The variation of maximum radial displacement versus the power law index for opening angles of $\frac{\pi}{18}$, $\frac{\pi}{4}$, $\frac{\pi}{2}$ and $\frac{2\pi}{3}$ is shown in Figure (4-a) to (4-d). It is observed that increasing the power law index increases the radial displacement where it is more intense when $P < 2$. Also increasing the opening angle and the nonlocal parameter tends to increase the radial displacement as seen in **Table 9**.

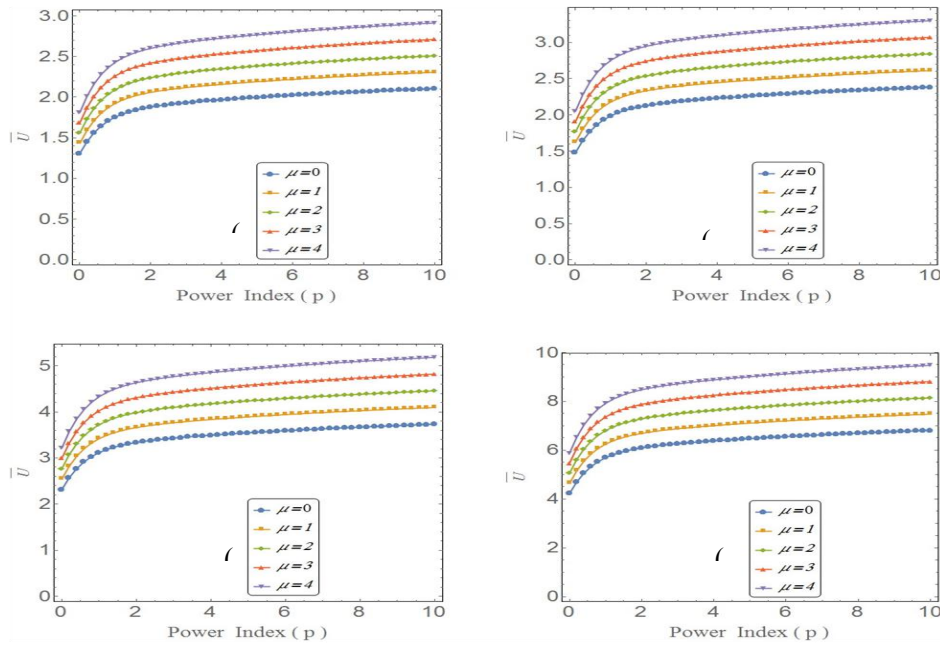


Figure 4; The variation of dimensionless radial deflection versus power law index for different nonlocal parameters of 0, 1, 2, 3 and 4 (nm^2), the opening angles of $\frac{\pi}{18}$ (a), $\frac{\pi}{4}$ (b), $\frac{\pi}{2}$ (c) and $\frac{2\pi}{3}$ (d).

The tangential displacements of curved FG nanobeam which is under the uniform load per the aforementioned parameters in Table 9 are represented in **Table 10**. The dimensionalized tangential displacement can be obtained by $\bar{w}_n = \frac{100E_c I}{f_0 R^4 \alpha^4} w_n(0)$. As seen, the tangential displacement increases with increasing the opening angle of the nanobeam which is more intense for $\alpha > \pi/2$ (or when $L/h = 50$). As the nonlocal parameter increases the tangential displacement increases. Comparing the table (9) and (10) it is resulted that the tangential displacement for the slight angles of curved FG nanobeam opening angle is negligible. It is due to this fact that for slight opening angles the mechanical behavior of curved FG nanobeam is close to those of straight one.

According to this fact there is negligible tangential displacement when the curved FG nanobeam is under the transverse load which tends to increase when the opening angle increases.

The variation of tangential displacements displacement versus power index law for different values of nonlocal parameter and opening angles of $\frac{\pi}{18}$, $\frac{\pi}{4}$, $\frac{\pi}{2}$ and $\frac{2\pi}{3}$ are shown in Figure (5-a) to (5-d). It is clear that as the power index

law increases the tangential displacement increase which reaches to zero when the power index law extends to infinity.

12. Conclusion

The free vibration and bending of a curved FG nanobeam utilizing the nonlocal theory is analyzed in this work. The differential equations and boundary conditions were obtained using the Hamilton principle. The nonlocal Euler-Bernoulli beam theory for a curved FG nanobeam was employed. Considering simply supported boundary conditions, an analytical solution is utilized and the opening angle of curved nanobeam, the power index law of FGM, the effect of nonlocal parameter and aspect ratio on dimensionless frequency, the radial and tangential dimensionless displacements are studied. The results revealed that as the radius of curved FG nanobeam extends to infinity the frequency of curved FG nanobeam approaches to those of straight nanobeam. Increasing the opening angle of curved nanobeam tends to increase the amount of natural frequencies and decrease the amount of radial and tangential displacements. This indicates the considerable influence of curved nanobeam opening angle on the aforementioned parameters. It was also concluded that as the nonlocal parameter increases the natural frequencies decrease and the amount of radial and tangential displacements increases which implies the importance of nonlocal theory in nanoscale in compared with classical theories.

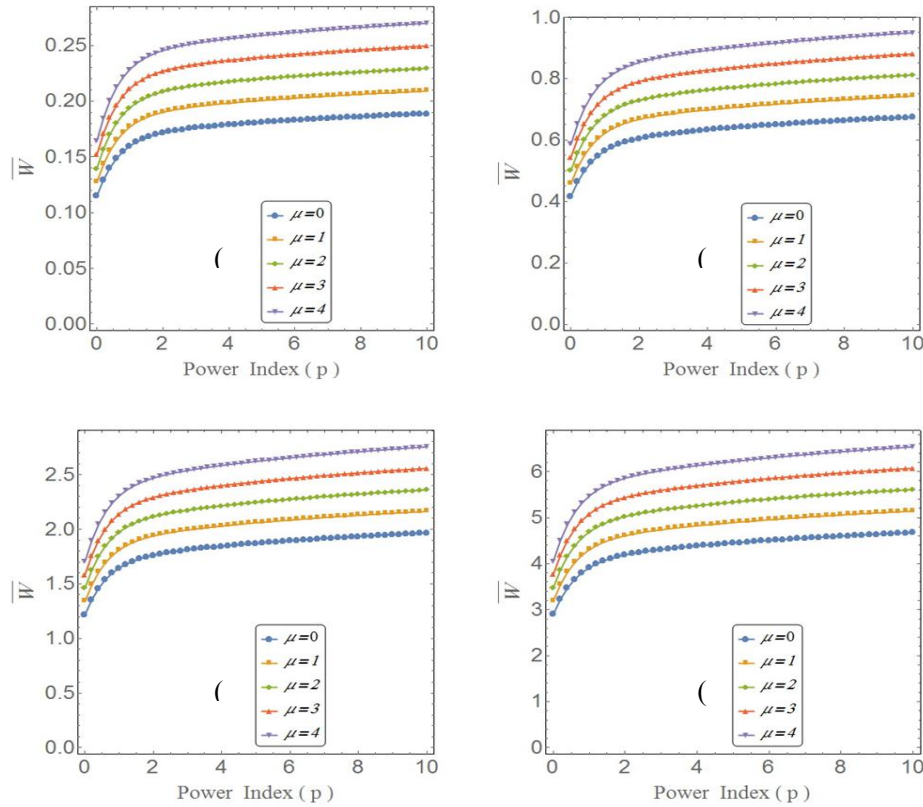


Figure 5; The variation of dimensionless tangential deflection versus power law index for different nonlocal parameters of 0, 1, 2, 3

and 4(nm^2), the opening angles of $\frac{\pi}{18}$ (a), $\frac{\pi}{4}$ (b), $\frac{\pi}{2}$ (c) and $\frac{2\pi}{3}$ (d).

p	$\mu(\text{nm}^{-2})$	opening angle (α)								
		$\frac{\pi}{18}$	$\frac{\pi}{9}$	$\frac{\pi}{6}$	$\frac{\pi}{4}$	$\frac{\pi}{3}$	$\frac{\pi}{2}$	$\frac{2\pi}{3}$	$\frac{3\pi}{4}$	
0	0	1.3101	1.3349	1.3778	1.4821	1.6492	2.3186	4.2300	6.8244	
		9	6	2	3	1	1	6	8	
	1	1.4359	1.4631	1.5102	1.6248	1.8083	2.5437	4.6436	7.4939	
		8	9	7	4	7	1	2	7	
	2	1.5617	1.5914	1.6427	1.7675	1.9675		5.0571	8.1634	
		8	2	2	6	3	2.7688	7	6	
	3	1.6875	1.7196	1.7751	1.9102	2.1266		5.4707	8.8329	
		8	6	7	7	9	2.9939	3	5	
	4	1.8133	1.8478	1.9076	2.0529	2.2858		5.8842	9.5024	
		8	9	2	9	5	3.219	9	4	
	0.1	0	1.3862	1.4125	1.4580	1.5685	1.7456	2.4546	4.4792	7.2272
			6	7	4	9	1	6	5	9
1		1.5193	1.5482		1.7196	1.9140	2.6929	4.9171		
		6	6	1.5982	3	7	7	7	7.9363	
2		1.6524	1.6839	1.7383	1.8706	2.0825	2.9312	5.3550	8.6453	
		7	5	6	7	3	8	9	1	
3		1.7855	1.8196	1.8785	2.0217		3.1695	5.7930	9.3543	
		7	4	2	1	2.251	8	1	2	
4		1.9186	1.9553	2.0186	2.1727	2.4194	3.4078	6.2309	10.063	
		7	3	8	5	6	9	3	3	
1		0	1.7565	1.7903		1.9894	2.2149	3.1171	5.6928	
			3	7	1.8485	8	1	7	9	9.1893
	1	1.9251	1.9623		2.1810	2.4286		6.2494	10.090	
		9	4	2.0262	5	7	3.4198	7	8	
	2	2.0938	2.1343	2.2038	2.3726	2.6424	3.7224	6.8060	10.992	
		4	2	9	1	2	2	4	3	
	3	2.2624		2.3815	2.5641	2.8561	4.0250	7.3626	11.893	
		9	2.3063	9	8	8	5	1	8	
	4	2.4311	2.4782	2.5592	2.7557	3.0699	4.3276	7.9191	12.795	
		5	8	9	5	3	7	9	2	
	10	0	2.1051	2.1453	2.2147	2.3831	2.6526	3.7316	6.8123	10.994
			1	6	2	4	3	6	5	1
1		2.3072	2.3514	2.4276	2.6126	2.9086	4.0939	7.4783	12.072	
		4	4	2	1	3	4	7	6	
2		2.5093	2.5575	2.6405	2.8420	3.1646	4.4562	8.1443	13.151	
		6	2	2	8	2	3	9	1	
3		2.7114		2.8534	3.0715	3.4206	4.8185	8.8104	14.229	
		8	2.7636	2	5	2	1	1	7	
4			2.9696	3.0663	3.3010	3.6766	5.1807	9.4764	15.308	
		2.9136	8	2	3	2	9	3	2	

Table 9. The variation of dimensionless radial displacement versus opening angle, nonlocal parameter and power law index for simply supported curved beam ($L/h=50$)

p	$\mu(\text{nm}^2)$	opening angle (α)								
		$\frac{\pi}{18}$	$\frac{\pi}{9}$	$\frac{\pi}{6}$	$\frac{\pi}{4}$	$\frac{\pi}{3}$	$\frac{\pi}{2}$	$\frac{2\pi}{3}$	$\frac{3\pi}{4}$	
0	0	0.11499	0.1913	0.2737	0.4168	0.5990	1.2186	2.9002	5.2195	
		1	29	13	1	71	3	2	2	
	1	0.1273	0.2112	0.3018	0.4592	0.6596	1.3406	3.1886	5.737	
		03	71	84	53	55	8			
	2	0.1396	0.2312	0.3300	0.5016	0.7202	1.4627	3.4769	6.2544	
		15	14	55	95	39	4	8	9	
	3	0.1519	0.2511	0.3582	0.5441	0.7808	1.5847	3.7653	6.7719	
		27	56	25	38	23	9	7	8	
	4	0.1642	0.2710	0.3863	0.5865	0.8414	1.7068	4.0537	7.2894	
		39	99	96	8	07	5	5	6	
	0.1	0	0.1225	0.2033	0.2905	0.4420	0.6351	1.2913	3.0726	5.5296
			88	8	87	95	06	3	7	2
		1	0.1357	0.2245	0.3205	0.4871	0.6993	1.4206	3.3782	6.0778
			25	92	1	28	51	9	2	7
		2	0.1488	0.2458	0.3504	0.5321	0.7635	1.5500	3.6837	6.6261
			62	05	33	61	95	4	7	2
3		0.1619	0.2670	0.3803	0.5771	0.8278	1.6794	3.9893	7.1743	
		99	17	55	95	4		2	7	
4		0.1751	0.2882	0.4102	0.6222	0.8920	1.8087	4.2948	7.7226	
		36	3	78	28	85	6	7	2	
1		0	0.1597	0.2622	0.3729	0.5653	0.8107	1.6456	3.9129	7.0405
			57	32	27	93	67	4	5	5

References

1. Kiani, K., *Small-scale effect on the vibration of thin nanoplates subjected to a moving nanoparticle via nonlocal continuum theory*. Journal of Sound and Vibration, 2011. 330(20): p. 4896-4914.
2. Soltani, P., et al., *Vibration of wavy single-walled carbon nanotubes based on nonlocal Euler Bernoulli and Timoshenko models*. International Journal of Advanced Structural Engineering (IJASE), 2012. 4(1): p. 1-10.
3. Hosseini-Hashemi, S., et al., *Surface effects on free vibration of piezoelectric functionally graded nanobeams using nonlocal elasticity*. Acta Mechanica, 2014. 225(6): p. 1555-1564.
4. Niknam, H. and M. Aghdam, *A semi analytical approach for large amplitude free vibration and buckling of nonlocal FG beams resting on elastic foundation*. Composite Structures, 2015. 119: p. 452-462.
5. Rahmani, O. and O. Pedram, *Analysis and modeling the size effect on vibration of functionally graded nanobeams based on nonlocal Timoshenko beam theory*. International Journal of Engineering Science, 2014. 77: p. 55-70.
6. Hosseini, S. and O. Rahmani, *Exact solution for axial and transverse dynamic response of functionally graded nanobeam under moving constant load based on nonlocal elasticity theory*. Meccanica, 2017. 52(6): p. 1441-1457.
7. Hosseini, S.A.H. and O. Rahmani, *Free vibration of shallow and deep curved FG nanobeam via nonlocal Timoshenko curved beam model*. Applied Physics A, 2016. 122(3): p. 1-11.
8. Hosseini, S.A.H. and O. Rahmani, *Thermomechanical vibration of curved functionally graded nanobeam based on nonlocal elasticity*. Journal of Thermal Stresses, 2016. 39(10): p. 1252-1267.
9. Sourki, R. and S.A. Hosseini, *Coupling effects of nonlocal and modified couple stress theories incorporating surface energy on analytical transverse vibration of a weakened nanobeam*. The European Physical Journal Plus, 2017. 132(4): p. 184.
10. Rahmani, O., et al., *Torsional Vibration of Cracked Nanobeam Based on Nonlocal Stress Theory with Various Boundary Conditions: An Analytical Study*. International Journal of Applied Mechanics, 2015. 07(03): p. 1550036.
11. Rahmani, O., et al., *Dynamic response of a double, single-walled carbon nanotube under a moving nanoparticle based on modified nonlocal elasticity theory considering surface effects*. Mechanics of Advanced Materials and Structures, 2017. 24(15): p. 1274-1291.
12. Rahmani, O., V. Refaieejad, and S. Hosseini, *Assessment of various nonlocal higher order theories for the bending and buckling behavior of functionally graded nanobeams*. Steel and Composite Structures, 2017. 23(3): p. 339-350.

13. Rahmani, O., et al., *Dynamic response of a single-walled carbon nanotube under a moving harmonic load by considering modified nonlocal elasticity theory*. The European Physical Journal Plus, 2018. 133(2): p. 42.
14. Ebrahimi, F. and E. Salari, *Nonlocal thermo-mechanical vibration analysis of functionally graded nanobeams in thermal environment*. Acta Astronautica, 2015. 113: p. 29-50.
15. Nazemnezhad, R. and S. Hosseini-Hashemi, *Nonlocal nonlinear free vibration of functionally graded nanobeams*. Composite Structures, 2014. 110: p. 192-199.
16. Salehipour, H., H. Nahvi, and A. Shahidi, *Exact analytical solution for free vibration of functionally graded micro/nanoplates via three-dimensional nonlocal elasticity*. Physica E: Low-dimensional Systems and Nanostructures, 2015. 66: p. 350-358.
17. Eltaher, M., A.E. Alshorbagy, and F. Mahmoud, *Vibration analysis of Euler–Bernoulli nanobeams by using finite element method*. Applied Mathematical Modelling, 2013. 37(7): p. 4787-4797.
18. Eltaher, M., S.A. Emam, and F. Mahmoud, *Static and stability analysis of nonlocal functionally graded nanobeams*. Composite Structures, 2013. 96: p. 82-88.
19. Eltaher, M., et al., *Static and buckling analysis of functionally graded Timoshenko nanobeams*. Applied Mathematics and Computation, 2014. 229: p. 283-295.
20. Uymaz, B., *Forced vibration analysis of functionally graded beams using nonlocal elasticity*. Composite Structures, 2013. 105: p. 227-239.
21. KANANIPOUR, H., I. KERMANI, and H. CHAVOSHI, *Nonlocal beam model for dynamic analysis of curved nanobeams and rings*.
22. Wang, C.M. and W. Duan, *Free vibration of nanorings/arches based on nonlocal elasticity*. Journal of Applied Physics, 2008. 104: p. 014303.
23. Farshi, B., A. Assadi, and A. Alinia-Ziazi, *Frequency analysis of nanotubes with consideration of surface effects*. Applied Physics Letters, 2010. 96: p. 093105.
24. Medina, L., R. Gilat, and S. Krylov, *Symmetry breaking in an initially curved micro beam loaded by a distributed electrostatic force*. International Journal of Solids and Structures, 2012. 49: p. 1864-1876.
25. Eringen, A.C. and D. Edelen, *On nonlocal elasticity*. International Journal of Engineering Science, 1972. 10(3): p. 233-248.
26. Eltaher, M., S.A. Emam, and F. Mahmoud, *Free vibration analysis of functionally graded size-dependent nanobeams*. Applied Mathematics and Computation, 2012. 218(14): p. 7406-7420.